Published in final edited form as:
Am J Geriatr Psychiatry. 2011 December ; 19(12): 1016–1025. doi:10.1097/JGP.0b013e318227f83f.

Serotonin Transporter Occupancy and the Functional Neuroanatomic Effects of Citalopram in Geriatric Depression

Gwenn S. Smith[1,2], **Alan Kahn**[1,2], **Julia Sacher**[1,2], **Pablo Rusjan**[1], **Thilo van Eimeren**[3], **Alastair Flint**[2,4], and **Alan A. Wilson**[1,2]

[1]PET Centre, Centre for Addiction and Mental Health (CAMH), University of Toronto Faculty of Medicine, Ontario, Canada

[2]Department of Psychiatry, University of Toronto Faculty of Medicine, Ontario, Canada

[3]Department of Neurology, University Health Network Toronto, Ontario, Canada

[4]Department of Psychiatry, University Health Network Toronto, Ontario, Canada

Abstract

Objectives—The functional neuroanatomic changes associated with selective serotonin reuptake inhibitor (SSRI) treatment have been the focus of positron emission tomography (PET) studies of cerebral glucose metabolism in geriatric depression.

Design—To evaluate the underlying neurochemical mechanisms, the present study measured both cerebral glucose metabolism and serotonin transporter (SERT) availability prior to and during treatment with the SSRI, citalopram. It was hypothesized that SERT occupancy would be observed in cortical and limbic brain regions that have shown metabolic effects, as well as striatal and thalamic regions that have been implicated in prior studies in mid-life patients.

Setting—Psychiatric Outpatient Clinic.

Participants—Seven depressed patients who met DSM-IV criteria for current major depressive episode were enrolled.

Intervention—Patients underwent a twelve week open-label trial of the SSRI, citalopram.

Measurements—Patients underwent high resolution research tomography (HRRT) PET scans to measure changes in cerebral glucose metabolism and SERT occupancy by citalopram treatment (after 8–10 weeks of treatment).

Results—Three different tracer kinetic models were applied to the [^{11}C]-DASB region of interest data and yielded similar results of an average of greater than 70% SERT occupancy in the striatum and thalamus during citalopram treatment. Voxel-wise analyses showed significant SERT occupancy in these regions, as well as cortical (e.g. anterior cingulate, superior and middle frontal, precuneus, and limbic (parahippocampal gyrus) areas that also showed reductions in glucose metabolism.

Conclusions—The findings suggest that cortical and limbic SERT occupancy may be an underlying mechanism for the regional cerebral metabolic effects of citalopram in geriatric depression.

Please address all correspondence and reprint requests to: Gwenn S. Smith, Ph.D., Division of Geriatric Psychiatry and Neuropsychiatry, Johns Hopkins University School of Medicine, Johns Hopkins Bayview Medical Center, 5300 Alpha Commons Drive, Fourth Floor, Baltimore, MD 21224, 410-550-8696 (phone), 410-550-0714 (fax), gsmith95@jhmi.edu.

Keywords

selective serotonin reuptake inhibitors; citalopram; serotonin; Positron Emission Tomography (PET); glucose metabolism; serotonin transporter; depression; aging

OBJECTIVES

Neuroimaging studies to evaluate the neurobiological substrates of treatment response variability in geriatric depression have employed positron emission tomography (PET) scans of cerebral glucose metabolism. These studies have measured alterations in functional circuitry underlying the response to antidepressant interventions, including total sleep deprivation (TSD) and selective serotonin reuptake inhibitor (SSRI) treatment (e.g. 1–4). These studies have implicated cortico-cortico and cortico-limbic pathways in the effects of antidepressant medications and correlations with treatment response in similar regions. The regions consistently implicated include the anterior cingulate, superior and middle frontal gyrus, precuneus and inferior parietal lobule. The underlying neurochemical mechanisms of the metabolic effects have not yet been a focus of study. Several lines of evidence indicate that the logical first step for such studies is the serotonin transporter (SERT).

SERT is the initial binding site of the SSRI's. SERT occupancy by SSRIs has been evaluated in controls and mid-life depressed patients (5,6). Studies in mid-life depressed patients treated for four weeks with citalopram, fluoxetine, sertraline, paroxetine, or extended-release venlafaxine have reported significant SERT occupancy in caudate, putamen and thalamus, in addition to prefrontal and anterior cingulate cortices. For citalopram, the magnitude SERT occupancy was 81.4% ± 7.2 for the striatum and 72.3% ± 7.6 for thalamus (6). At this time, there do not appear to be any published studies of SERT occupancy in geriatric depression.

SERT is particularly relevant to the functional neuroanatomy of depression given its localization in cortical, striatal and limbic areas (7,8). Post-mortem autoradiographic studies in the human brain show that SERT densities are relatively higher in anterior cingulate, the subcallosal area, entorhinal and insular cortices, temporal pole, hippocampus (molecular layer and CA3 and external layers of the subiculum), caudate, putamen, thalamus and in the raphe nuclei. Based on the regional distribution, SERT has a potentially important modulatory role with respect to brain regions implicated in geriatric depression (4,9).

Thus, to evaluate the neurochemical mechanisms underlying the cerebral metabolic effects of SSRIs, the present study measured cerebral glucose metabolism and SERT availability before and during treatment with the SSRI, citalopram in geriatric depressed patients. The association between the magnitude of SERT occupancy, as well as alterations in cerebral glucose metabolism, and the clinical response to citalopram treatment was also evaluated. Please note that SERT availability refers to the measurement of SERT binding sites not occupied by drug and SERT occupancy refers to the change in available SERT binding sites between the treated and untreated states. The hypotheses were tested that 1) significant SERT occupancy would be observed in striatal and thalamic regions during citalopram treatment and 2) regional SERT occupancy in cortical and limbic areas would be similar to the regional pattern of cerebral metabolic alterations observed (anterior cingulate gyrus, precuneus, parahippocampal gyrus) and 3) that SERT occupancy and decreases in glucose metabolism in cortical and limbic regions would be associated with antidepressant response. These results have been presented in preliminary form (10).

METHODS

Study Design

Prior to starting citalopram treatment, patients underwent medical and psychiatric screening, a magnetic resonance (MR) imaging scan and two PET scans to measure cerebral glucose metabolism and SERT availability. Then, the patients began a twelve week treatment trial with citalopram. Eight to ten weeks after starting treatment (after achieving a stable clinical response for 2 weeks based on the Hamilton Depression Rating Scale score), the patients underwent the same PET protocol. The patients were re-scanned at this time based upon the observation from prior studies that this is the time by which patients should have demonstrated clinical improvement if they respond to antidepressant treatment (11).

Subject Screening and Selection

Patients underwent psychiatric evaluation (including a structured clinical interview, [SCID; 12]), laboratory testing (including CBC and blood chemistry, including glucose levels and thyroid function tests), toxicology screening and MR imaging scans (Siemens 3T Trio scanner) prior to the PET scans. Depressed patients were recruited from advertisements in the community.

Seven depressed patients (4 M/ 3 F, mean age 65 ± 5 years; modified mini mental status score (MMSE; 13) 29.1 ± 1.1 (range 27–30) who met DSM-IV criteria for current major depressive episode (non-bipolar, non-psychotic) were enrolled. Subjects who had a history of or current neurological or other Axis I psychiatric disorders including substance abuse, who were not medically stable (including a current diagnosis of insulin dependent diabetes and/or poorly controlled hypertension) or who had used prescription or over the counter medications (e.g. antihistamines, cold medications) with central nervous system effects within the past two weeks were excluded from the study. Five patients had never been treated with psychotropic drugs. The two patients previously treated had both taken amitriptyline in the past (two months and three years prior to study enrollment). After a complete description of the study to the subjects, written informed consent was obtained according to procedures established by the Research Ethics Boards of the Centre for Addiction and Mental Health, Baycrest Centre for Geriatric Care and the University Health Network.

Citalopram Treatment

After the baseline PET scans were completed, the patients began treatment with a 10 mg per day dose of citalopram for one week. Then, the dose was increased to 20mg. If significant clinical improvement was not observed at the 20mg dose after four weeks of treatment based on an improvement rating of 3 or greater on the Clinical Global Impression Scale (CGI, 14), the dose was increased to 30mg and then if necessary, to 40mg. Patients were followed clinically on a weekly basis at which time clinical ratings for depression and anxiety symptoms were performed (Hamilton Depression Rating Scale-24 item [HDRS; 15] and Hamilton Anxiety Rating Scale [HARS; 16], as well as the CGI. Plasma citalopram concentrations were determined every four weeks (17), including a sample obtained just prior to injection of the radiotracer for the second SERT PET scan.

Neuroimaging Procedures

MR scans were performed on a Siemens 3T Trio scanner at the Baycrest Centre for Geriatric Care. The PET scans were performed on the CPS/Siemens high resolution research tomography (HRRT) scanner at the Centre for Addiction and Mental Health. The PET radiotracer [^{11}C]-3-amino-4-(2-dimethylaminomethyl-phenylsulfanyl)-enzonitrile, ([^{11}C]-DASB) was used to measure SERT. [11C]-DASB was synthesized as described (18). For the

[^{11}C]-DASB scan, dynamic scanning began immediately upon a 10mCi ±10% radiotracer injection and lasted for 90 minutes. The cerebellum was used for the input function. Glucose metabolism was measured with [^{18}F]-2-deoxy-2-fluoro-D-glucose ([^{18}F]-FDG). [^{18}F]-FDG was synthesized as described (19,20). A similar scan protocol was used as in previous geriatric depression treatment studies (4,9). During the radiotracer uptake period and during scanning, subjects were maintained in a quiet, dimly lit room, with eyes open and ears unoccluded. 30 minutes after a 5mCi ± 10% radiotracer injection, patients were positioned in the scanner and a twenty minute emission scan was obtained, followed by a transmission scan. The last ten minutes of the emission scan were used for quantitative analysis. At the end of the PET scans sessions, the subjects were debriefed as to her/his perception of the study. The glucose metabolism and SERT PET scans were repeated 8–10 weeks after the patients started citalopram treatment. The follow-up PET scans were scheduled after a minimum of six weeks of treatment at a time when the patients demonstrated a stable clinical response (consistent HDRS scores) for two consecutive weeks.

Data and Image Analysis

For [^{11C}]-DASB, tracer kinetic modeling was performed on regions of interest (ROI) and parametric images of the distribution volume ratio (DVR) were calculated to be used in voxel-wise analyses. ROI analysis was performed using an automated analysis method that superimposed an ROI template on an MR scan and refined the ROI placement based on a probabilistic grey matter image extracted from the subjects' MR scan. The rigid body transformation for MR to PET co-registration was estimated and applied to the ROIs. The ROIs were then superimposed on the co-registered frames from the PET scans and a time activity curve was generated (Region of Mental Interest [ROMI]: 21). The regional time activity curves were analyzed with three different tracer kinetic modeling methods to determine whether the methods implemented in prior studies in younger subjects would be appropriate to use in older subjects. Three methods were used to calculate the binding potential (BP_{ND}) including the Logan graphical analysis method, the simplified reference tissue model (SRTM) and the multilinear reference tissue model [MRTM2] (as described in 22–24). The cerebellar ROI was used for the input function. The cerebellar ROI was carefully delineated to include the cerebellar grey matter and exclude the white matter and vermis as described in prior [^{11}C]-DASB studies (as reviewed by 25). Parametric [^{11}C]-DASB maps were calculated applying the Logan model in wavelet space in the following manner: (1) a wavelet transform was applied to each 3D spatial volume of the dynamic PET scans, (2) the linear regression for Logan model was estimated in the transformed-image to calculate the distribution volume ratio (DVR), (3) the DVR was transformed from the wavelet space to the real space (26,27).

Glucose metabolic rates were calculated (in ml/100g/min) on a pixel by pixel basis by using a single venous blood sample (obtained 20 minutes after radiotracer injection) that is fit to a population curve (4,9, 28). This quantification method has been validated against arterial blood sampling (28).

For both the [^{11}C]-DASB DVR parametric images and [^{18}F]-FDG quantitative images, PET to PET and MR to PET co-registration was performed with statistical parametric mapping, version 5 (SPM5, Institute of Neurology, London) using the normalized mutual information algorithm. Voxel-wise, statistical analyses were performed with SPM5. For the voxel-wise analyses, the glucose metabolism and parametric [^{11}C]-DASB DVR images were smoothed with an isotropic Gaussian kernel (FWHM 4mm). The glucose metabolic rates were normalized by scaling to a common mean value across all scans, after establishing that the global means did not differ significantly across conditions ($p > 0.1$). For the [^{11}C]-DASB and [^{18}F]-FDG data, a within-subject comparison of the baseline pretreatment to the chronic treatment condition was performed using the flexible factorial option (paired t-test) in SPM5

to evaluate the effects of citalopram on cerebral glucose metabolism and to measure SERT occupancy by citalopram. Then, the change in depressive symptoms (HDRS) score was correlated with the change in metabolism and also with SERT availability. The comparisons/correlations were considered significant at $z \geq 2.98$, $p \leq 0.00288$; two-tailed, uncorrected for multiple independent comparisons) and was reported if the cluster size (K_E) was greater than 50 voxels.

RESULTS

The HDRS scores were: baseline 20.6 ± 2.7 (range 17–25), second PET scan 7.7 ± 7.4 (range 0–21) and week 12 of treatment 7.6 ± 6.1 (range 0–15). 5/7 patients met criteria for treatment response (50% reduction from baseline) at the second PET scan session and 4/7 at 12 weeks of treatment. 4/7 met criteria for remission (HDRS below 8) at the second PET scan session and at 12 weeks of treatment. The HARS scores were: baseline 15.9 ±6.0, second PET scan 6.9 ± 6.7 and week 12 of treatment 7.7 ± 8.0 At the time of the second PET scan session, the mean citalopram dose was 27.1 ± 9.5 (range 20–40mg) and 12 weeks of treatment it was 25.7 ± 7.9 (range 20–40mg). The mean plasma citalopram concentrations were: week 4 110 ± 54nmol/L (range 61–222 nmol/L) and second PET scan (week 8–10) 148 ± 86nmol/L (range 72–294 nmol/L).

For the [^{11}C]-DASB data, the means and standard deviations for the baseline and the treatment scan and the percent SERT occupancy for the striatum and thalamus (100 X ($SERT_{baseline} - SERT_{citalopram\ treatment}$)/$SERT_{baseline}$; right and left hemispheres combined) determined by three tracer kinetic models is shown in Table 1. The results are similar for the three tracer kinetic models, as well as for the striatum and thalamus. Greater than 70% occupancy is observed for the striatum and thalamus. The magnitude of striatal or thalamic SERT occupancy was not significantly correlated with the degree of improvement in the HDRS or HARS score or with the plasma citalopram concentration, as shown in previous studies ($p>0.1$). These associations were comparable for results derived by all three tracer kinetic models.

The results of the voxel-wise analysis of changes in SERT availability with citalopram treatment are shown in Table 2. A parametric image from a representative subject is shown in Figure 1. The regions of significant SERT occupancy include anterior cingulate, superior middle and inferior frontal gyri (bilaterally), superior temporal gyrus (bilaterally), right middle temporal gyrus, left parahippocampal gyrus, precuneus (bilaterally), post-central gyrus (bilaterally), right cuneus, left brainstem and striatum (bilaterally). The results of the correlation between change in HDRS and SERT occupancy are shown in Table 3. Positive correlations were observed in many of the same regions including the anterior cingulate gyrus (bilaterally), left middle and inferior frontal gyrus, right superior and middle temporal gyrus, right precuneus, left inferior parietal lobule, parahippocampal gyrus (bilaterally) and left cuneus. Significant negative correlations were not observed ($p > 0.1$).

The results of the voxel-wise analysis of the glucose metabolism data for the comparison of baseline to treatment are shown in Table 4. Decreases in cerebral glucose metabolism with citalopram treatment were observed in anterior cingulate gyrus (bilaterally), medial and inferior frontal gyrus (bilaterally), insula (bilaterally), right superior temporal gyrus, middle and inferior temporal gyrus (bilaterally), parahippocampal gyrus (bilaterally), precuneus (bilaterally), posterior cingulate gyrus (bilaterally). Increases in cerebral glucose metabolism with citalopram treatment were observed in pre-central gyrus (bilaterally), caudate and putamen (bilaterally), left inferior parietal lobule, right middle occipital gyrus. The results of the correlation between change in HDRS and glucose metabolism are shown in Table 5. Positive correlations were observed in the left cingulate gyrus (BA 24), right pre-central,

right medial frontal, right superior, middle and inferior temporal gyri, left fusiform gyrus and precuneus (bilaterally). Negative correlations are observed in the superior parietal lobule (left), inferior parietal lobule (bilaterally) and right cuneus.

CONCLUSIONS

In the present study, 71% of patients met criteria for response (50% or greater reduction in HDRS score) and 57% for remission (HDRS score below 8) at the time of the second PET scan session during citalopram treatment. These rates of non-response are consistent with the results of randomized clinical trials of antidepressants in geriatric depression (29) as well as previous neuroimaging studies that involve “open label” treatment (1,2). During citalopram treatment, greater than 70% SERT occupancy in striatum and thalamus was observed. The results were consistent over the three tracer kinetic models evaluated. Significant SERT occupancy in striatum and thalamus was observed in the voxel-wise analysis, as well. The average percentage SERT occupancy for the group of patients is slightly lower for the striatum and comparable for the thalamus compared to SERT occupancy observed in mid-life depressed patients treated with SSRIs including citalopram (5,6). The lack of a significant correlation between SERT occupancy by SSRIs in striatum and thalamus and with either antidepressant response or plasma concentrations in the present study was also observed in a previous SSRI treatment study (including citalopram) in midlife depressed patients (6). These observations suggest, as reported in other studies, that SERT occupancy reaches a plateau at relatively low citalopram plasma levels (6) and that SERT occupancy in cortical and limbic brain regions are better associated with the antidepressant response.

Voxel-wise analyses of the parametric [^{11}C]-DASB images confirmed the ROI findings of significant SERT occupancy in striatum and thalamus, in addition to other cortical and limbic brain regions including the midbrain, anterior cingulate (BA24), middle frontal and middle temporal gyri and parahippocampal gyrus. Voxel-wise analyses revealed significant correlations between the change in HDRS score and SERT occupancy in cortical and limbic regions. The cerebral metabolic effects of citalopram observed in the present study are consistent with other studies in geriatric depressed patients using TSD, citalopram and paroxetine (1,3). While the results involving striatal and thalamic occupancy and the relationship to plasma citalopram concentrations is similar to data in mid-life depressed patients, the observations of the relationship between cortical and limbic occupancy and clinical response have not been reported in mid-life depressed patients. There is converging evidence from diffusion tensor imaging (DTI) and functional MR studies (as reviewed previously by 4,9), of alterations in the same regions that are associated with antidepressant responses that showed metabolic effects and SERT occupancy in the present study. For example, a recent DTI study revealed decreased white matter connectivity associated with poorer antidepressant response in many of the same regions shown in the present study to be affected by citalopram including the anterior and posterior cingulate, precuneus and hippocampus/parahippocampal gyrus (30). The cortical regions that show metabolic effects of chronic citalopram treatment, as well as SERT occupancy, are regions that have also shown consistent activation responses in a variety of conditions including mood induction, attention and memory tasks, and during conditions of hunger and satiety (31–33).

In the present study, SERT occupancy in cortical and limbic regions was correlated with antidepressant response. The present study differs from previous SERT occupancy studies in that SERT occupancy was measured after a longer duration of treatment to allow an antidepressant effect to be observed (more than 8 weeks of treatment as compared to 4 weeks in other studies), a voxel-wise analysis was used to evaluate SERT occupancy and

correlations with improvement in depressive symptoms in regions outside of the striatum and thalamus and the sample focusd on geriatric depressed patients.

There are several possible explanations for the mechanism underlying the correlation between the magnitude of SERT occupancy and clinical response. One possibility is that the concentration of SERT in these areas is reduced and there are fewer SERT binding sites to be occupied by citalopram. While there do not appear to be published PET studies of SERT in geriatric depression, the available post-mortem data has not shown a difference between geriatric depressed patients and age matched controls in SERT binding sites (34). PET studies are in progress to evaluate changes in SERT in geriatric depressed patients relative to age matched controls. A second possibility might that the lower occupancy reflects altered functional integrity of serotonergic projections to the cortex. Future studies will address this hypothesis by using a recently developed serotonin (5-HT1A) receptor agonist (e.g. [^{11}C]-CUMI 101) that binds to high affinity 5-HT1A sites and has been shown to be sensitive to changes in endogenous serotonin (35). Given the widespread localization and functional role of the 5-HT1A receptor, the effects of citalopram displacement of the 5-HT1A agonist binding site would provide important information regarding the functional integrity of the cortical and limbic serotonin projections.

Several issues should be considered in the interpretation of the findings from this study. The sample size is relatively small (n=7) as it was extremely challenging to recruit a mostly never medicated, medically stable group of geriatric depressed patients. It is important to note that the results obtained for the two subjects who had been treated previously with antidepressants did not differ significantly from the rest of the group. The second issue is the lack of a placebo control group, as changes in cerebral glucose metabolism similar to those observed with antidepressant treatment have been observed in placebo treated patients in pharmacologic treatment studies (36). While we cannot rule out the effects of placebo response, it is important to note the rate of treatment non-response observed in the study was similar to that observed in placebo controlled antidepressant clinical trials in geriatric depression (28). The present findings should be replicated in a larger sample size of patients.

A third consideration is that the regional SERT occupancy measurements may be affected by changes in cerebral blood flow secondary to citalopram treatment that would result in decreased radiotracer delivery to specific brain regions. It is important to note that SERT occupancy and correlations with HDRS were observed in regions that show decreases as well as increases in glucose metabolism. While cerebral blood flow was not measured directly in this study, metabolism and blood flow have been shown to be coupled during citalopram administration (37). Finally, the cerebellum was used for the input function rather than obtaining an arterial input function. It has been suggested that since there is some degree of specific binding to SERT in the cerebellum, the use of the cerebellum as the input function may underestimate the results (38,39). In fact, the comparison of SERT occupancy using arterial versus cerebellar input functions demonstrates that the magnitude of SERT occupancy with [^{11}C]-DASB is similar for both input function methods (25).

In summary, changes in cerebral glucose metabolism and SERT occupancy by citalopram in cortico-cortico and cortico-limbic pathways are associated with improvement in depressive symptoms. Future studies will apply this multi-tracer methodology to a larger patient sample to determine the relationship of these metabolic and neurochemical mechanisms relative to improvement of mood, anxiety and cognitive symptoms in geriatric depressed patients.

Acknowledgments

Supported in part by National Institute of Health: MH64823 (GSS) and MH01621 (GSS). Alvina Ng, Jeannie Fong, Armando Garcia, Jun Parkes, Peter Bloomfeld, Terry Bell, Ted Harris-Brandts are gratefully acknowledged for

their contribution to the acquisition and analysis of the HRRT PET studies and Annette Weeks-Holder for the conduct of the MR studies. The results were reported in preliminary form at the Seventh International Symposium on Functional Neuroreceptor Mapping of the Living Brain, July 17–19, 2009, Pittsburgh, Pennsylvania. This manuscript is dedicated to Tatiana Jasmine Rusjan.

References

1. Diaconescu A, Kramer E, Hermann C, Ma Y, et al. The functional neuroanatomy of recovery of affective symptoms and cognitive deficits in geriatric depression. Human Brain Mapping. 2011 in press.
2. Smith G, Kramer E, Hermann C, Goldberg S, et al. Serotonin Modulation of Cerebral Glucose Metabolism in Geriatric Depression. American Journal of Geriatric Psychiatry. 2002a; 10:715–723. [PubMed: 12427580]
3. Smith G, Reynolds C, Houck P, Dew M, et al. The Glucose Metabolic Response to Total Sleep Deprivation, Recovery Sleep and Acute Antidepressant Treatment as Functional Neuroanatomic Correlates of Treatment Outcome in Geriatric Depression. American Journal of Geriatric Psychiatry. 2002b; 10(5):561–567. [PubMed: 12213690]
4. Smith G, Kramer E, Hermann C, Ma Y, Kingsley P, et al. The functional neuroanatomy of geriatric depression. International Journal of Geriatric Psychiatry. 2009b; 24:798–808. [PubMed: 19173332]
5. Meyer JH, Wilson AA, Ginovart N, Goulding V, et al. Occupancy of SERTs by paroxetine and citalopram during treatment of depression: a [(11)C]DASB PET imaging study. American Journal of Psychiatry. 2001; 158(11):1843–9. [PubMed: 11691690]
6. Meyer JH, Wilson AA, Sagrati S, Hussey D, et al. Serotonin transporter occupancy of five selective serotonin reuptake inhibitors at different doses: an [^{11}C]DASB positron emission tomography study. American Journal of Psychiatry. 2004; 161(5):826–35. [PubMed: 15121647]
7. Steinbusch H. Distribution of serotonin immunoreactivity in the central nervous system of the rat. Neuroscience. 1981; 6:557–618. [PubMed: 7017455]
8. Varnäs K, Halldin C, Hall H. Autoradiographic distribution of serotonin transporters and receptor subtypes in human brain. Human Brain Mapping. 2004; 22(3):246–60. [PubMed: 15195291]
9. Smith G, Kramer E, Hermann C, Ma Y, et al. Serotonin modulation of cerebral glucose metabolism in geriatric depression. Biological Psychiatry. 2009a; 66(3):259–66. [PubMed: 19368900]
10. Smith G, Kahn A, Hanratty K, Sacher J, et al. Serotonin Transporter Occupancy by Citalopram Treatment in Geriatric Depression. Neuroimage. 2008; 41 (2):T168.
11. Sackeim HA, Roose SP, Lavori PW. Determining the duration of antidepressant treatment: application of signal detection methodology and the need for duration adaptive designs (DAD). Biological Psychiatry. 2006; 59(6):483–92. [PubMed: 16517241]
12. First, M.; Spitzer, R.; Gibbon, M.; Williams, J. Structured clinical interview for DSM-IV axis 1 disorders-patient edition (SCID-I/P). New York: New York Psychiatric Institute; 1995.
13. Folstein M, Folstein S, McHugh P. Mini-mental state. Journal of Psychiatric Research. 1976; 12:189–198. [PubMed: 1202204]
14. National Institute of Mental Health. Clinical global impressions. In: Guy, W.; Bonato, RR., editors. Manual for the ECDEU assessment battery. 2. Rockville, MD: National Institute of Mental Health; 1976.
15. Hamilton M. A rating scale for depression. Journal of Neurology, Neurosurgery and Psychiatry. 1960; 23:56–62.
16. Hamilton M. The assessment of anxiety states by rating. British Journal of Medical Psychology. 1959; 32:50–55. [PubMed: 13638508]
17. Foglia JP, Pollock BG, Kirshner MA, Rosen J, et al. Plasma levels of citalopram enantiomers and metabolites in elderly Patients. Psychopharmacology Bulletin. 1997; 33(1):109–12. [PubMed: 9133760]
18. Wilson AA, Ginovart N, Hussey D, Meyer J, Houle S. In vitro and in vivo characterization of [^{11}C]-DASB: a probe for in vivo measurements of the serotonin transporter by positron emission tomography. Nuclear Medicine and Biology. 2002; 29(5):509–15. [PubMed: 12088720]

19. Hamacher K, Coenen H, Stöcklin G. Efficient Stereospecific Synthesis of No-Carrier-Added 2-[^{18}F]-Fluoro-2-Deoxy-D-Glucose Using Aminopolyether Supported Nucleophilic Substitution. Journal of Nuclear Medicine. 1986; 27:235–238. [PubMed: 3712040]
20. Lemaire C, Damhaut B, Lauricella C, Mosdzianowski JL, et al. Fast [^{18}F]FDG synthesis by alkaline hydrolysis on a low polarity solid phase support. Journal of Labelled Compounds and Radiopharmaceuticals. 2002; 45:435–47.
21. Rusjan P, Mamo D, Ginovart N, Hussey D, et al. An automated method for the extraction of regional data from PET images. Psychiatry Research. 2006; 147(1):79–89. [PubMed: 16797168]
22. Ginovart N, Wilson AA, Meyer JH, Hussey D, et al. Positron emission tomography quantification of [(11)C]-DASB binding to the human serotonin transporter: modeling strategies. Journal of Cerebral Blood Flow and Metabolism. 2001; 21(11):1342–53. [PubMed: 11702049]
23. Frankle WG, Slifstein M, Gunn RN, Huang Y, et al. Estimation of serotonin transporter parameters with ^{11}C -DASB in healthy humans: reproducibility and comparison of methods. Journal of Nuclear Medicine. 2006; 47(5):815–26. [PubMed: 16644752]
24. Kim JS, Ichise M, Sangare J, Innis RB. PET imaging of serotonin transporters with [^{11}C]DASB: test-retest reproducibility using a multilinear reference tissue parametric imaging method. Journal of Nuclear Medicine. 2006; 47(2):208–14. [PubMed: 16455625]
25. Parsey RV, Kent JM, Oquendo MA, Richards MC, et al. Acute occupancy of brain serotonin transporter by sertraline as measured by [^{11}C]DASB and positron emission tomography. Biological Psychiatry. 2006; 59(9):821–8. [PubMed: 16213473]
26. Cselényi Z, Olsson H, Farde L, Gulyás B. Wavelet-aided parametric mapping of cerebral dopamine D2 receptors using the high affinity PET radioligand [^{11}C]FLB 457. Neuroimage. 2002; 17(1):47–60. [PubMed: 12482067]
27. Turkheimer FE, Banati RB, Visvikis D, Aston JA, et al. Modeling dynamic PET-SPECT studies in the wavelet domain. Journal of Cerebral Blood Flow and Metabolism. 2000; 20(5):879–93. [PubMed: 10826539]
28. Takikawa S, Dhawan V, Spetsieris P, Robeson W, et al. Noninvasive quantitative fluorodeoxyglucose PET studies with an estimated input function derived from a population-based arterial blood curve. Radiology. 1993; 188(1):131–6. [PubMed: 8511286]
29. Little JT, Reynolds CF 3rd, Dew MA, Frank E, et al. How common is resistance to treatment in recurrent, nonpsychotic geriatric depression? American Journal of Psychiatry. 1998; 155(8):1035–8. [PubMed: 9699690]
30. Alexopoulos GS, Murphy CF, Gunning-Dixon FM, Latoussakis V, et al. Microstructural white matter abnormalities and remission of geriatric depression. American Journal of Psychiatry. 2008; 165(2):238–44. [PubMed: 18172016]
31. Fletcher PC, Frith CD, Baker SC, Shallice T, et al. The mind's eye--precuneus activation in memory-related imagery. Neuroimage. 1995; 2(3):195–200. [PubMed: 9343602]
32. Liotti M, Mayberg HS, Brannan SK, McGinnis S, et al. Differential limbic-cortical correlates of sadness and anxiety in healthy subjects: implications for affective disorders. Biological Psychiatry. 2000; 48(1):30–42. [PubMed: 10913505]
33. Tataranni PA, Gautier JF, Chen K, Uecker A, et al. Neuroanatomical correlates of hunger and satiation in humans using positron emission tomography. Proceeding of the National Academy of Sciences. 1999; 96(8):4569–4574.
34. Thomas AJ, Hendriksen M, Piggott M, Ferrier IN, et al. A study of the serotonin transporter in the prefrontal cortex in late-life depression and Alzheimer's disease with and without depression. Neuropathology and Applied Neurobiology. 2006; 32(3):296–303. [PubMed: 16640648]
35. Milak M, Kumar JSD, Severance AJ, Ogden RT, et al. Altered binding in baboons of [^{11}C]CUMI-101, a 5-HT$_{1A}$ agonist PET tracer, in response to intravenous citalopram. Neuroimage. 2008; 41(S2):T162.
36. Mayberg HS, Silva JA, Brannan SK, Tekell JL, et al. The functional neuroanatomy of the placebo effect. American Journal of Psychiatry. 2002; 159(5):728–37. [PubMed: 11986125]
37. McBean D, Ritchie I, Olverman H, Kelly P. Effects of the specific serotonin reuptake inhibitor, citalopram, upon local cerebral blood flow and glucose utilization in the rat. Brain Research. 1999; 847(1):80–84. [PubMed: 10564738]

38. Hinz R, Selvaraj S, Murthy NV, Bhagwagar Z, Taylor M, Cowen PJ, Grasby PM. Effects of citalopram infusion on the serotonin transporter binding of [^{11}C]DASB in healthy controls. Journal of Cerebral Blood Flow and Metabolism. 2008; 28(8):1478–90. [PubMed: 18478022]

39. Kish SJ, Furukawa Y, Chang LJ, Tong J, et al. Regional distribution of serotonin transporter protein in postmortem human brain: is the cerebellum a SERT-free brain region? Nuclear Medicine and Biology. 2005; 32(2):123–8. [PubMed: 15721757]

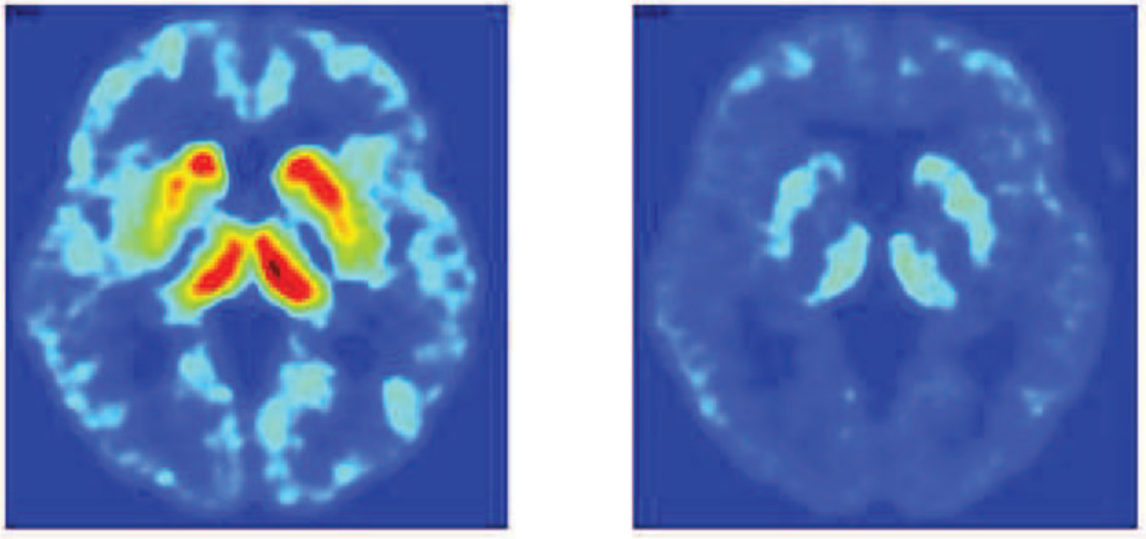

Figure 1.
Changes in Serotonin Transporter Availability by Chronic Citalopram Treatment: Parametric [^{11}C]-DASB DVR images at the level of the striatum, prior to (left) and during (right) citalopram treatment for a representative subject 68 year old elderly depressed male patient.

Table 1

SERT Occupancy in Striatum and Thalamus: Comparison of Three Tracer Kinetic Models for [^{11} C]-DASB (BP_{ND})

Striatum			
	PRE	**POST**	**% OCC**
Logan	1.46 ±.34	0.38±.06	73 ± 5
(range)	1.14–1.98	0.28–0.45	67–80
SRTM	1.43 ± 0.25	0.34± 0.6	73 ±5
(range)	1.17–1.82	0.29–0.45	65–79
MRTM2	1.42 ± 0.22	0.40 ± 0.04	71 ± 5
(range)	1.20–1.78	0.32–0.44	66–77

Thalamus			
	PRE	**POST**	**% OCC**
Logan	1.77±0.45	0.43±0.11	75 ± 7
(range)	0.99– 2.57	0.25–0.58	66–85
SRTM	1.93 ± 0.62	0.44 ± 0.12	76 ± 5
(range)	1.07–2.86	0.22–0.62	68–84
MRTM2	1.71 ± 0.44	0.46 ± 0.09	72 ± 6
(range)	0.99–2.26	.33 – .66	65–81

Table 2

Changes in SERT Availability During Citalopram Treatment.

DECREASE		Left Hemisphere					Right Hemisphere	
	Talairach Coordinates					Talairach Coordinates		
x (mm)	y (mm)	z (mm)	Z score	Structure	x (mm)	Y (mm)	z (mm)	Z score
−12	−28	37	3.11	Anterior Cingulate Gyrus	4	−4	45	3.28
−20	59	17	2.98	Superior Frontal Gyrus	28	58	−4	4.17
−37	45	26	3.78	Middle Frontal Gyrus (BA 6)	36	55	−2	3.46
−41	15	−9	4.39	Inferior Frontal Gyrus (BA 6)	23	31	−9	3.9
−46	10	−5	3.00	Superior Temporal Gyrus	54	−17	5	3.37
−53	−36	−10	2.99	Middle Temporal Gyrus	47	−75	16	3.99
−51	−33	−17	3.32	Parahippocampal Gyrus				
				Post-central Gyrus	48	−20	57	3.68
				Precuneus	10	−50	62	3.67
				Cuneus	11	−91	13	4.85
−10	−26	−3	6.47	Brainstem				
−18	1	2	6.11	Lentiform Nucleus	30	−3	−1	5.87
INCREASE		Left Hemisphere					Right Hemisphere	
−56	−14	32	3.29	Pre-Central Gyrus	52	−1	30	4.68
−12	7	12	3.30	Caudate	8	6	16	3.29
−17	6	−10	3.01	Putamen	31	−11	−3	3.75
−56	−23	33	4.04	Inferior Parietal Lobule				
				Middle Occipital Gyrus	38	−77	1	2.99

Note: For all Tables, the coordinates shown are all significant at $z \geq 2.98$, $p \leq 0.00288$.

Table 3

Positive Correlations between Change in SERT Availability During Citalopram Treatment and Hamilton Depression Rating Scale (HDRS) Ratings

POSITIVE		Left Hemisphere					Right Hemisphere	
	Talairach Coordinates					Talairach Coordinates		
x (mm)	y (mm)	z (mm)	Z score	Structure	x (mm)	y (mm)	z (mm)	Z score
−3	−6	27	3.36	Anterior Cingulate Gyrus	15	−16	35	4.08
−31	49	−11	3.58	Middle Frontal Gyrus (BA 6)				
−54	33	3	3.46	Inferior Frontal Gyrus (BA 6)				
				Superior Temporal Gyrus	61	2	1	3.32
				Middle Temporal Gyrus	39	−72	25	3.47
−19	−8	−16	3.62	Parahippocampal Gyrus	36	−23	−25	2.99
				Precuneus	3	−59	49	3.68
−39	−50	43	73.48	Inferior Parietal Lobule				
				Cuneus	12	−98	12	3.19

Table 4

Change in Cerebral Glucose Metabolism with Citalopram Treatment

DECREASE		Left Hemisphere					Right Hemisphere	
	Talairach Coordinates					Talairach Coordinates		
x (mm)	y (mm)	z (mm)	Z score	Structure	x (mm)	y (mm)	z (mm)	Z score
−7	46	8	3.57	Anterior Cingulate Gyrus	9	−22	37	3.52
−36	29	29	3.20	Middle Frontal Gyrus	9	47	10	3.03
−31	31	−4	3.64	Inferior Frontal Gyrus (BA 6)	31	22	−6	2.99
−41	2	14	3.07	Insula	34	−6	13	3.60
				Superior Temporal Gyrus	40	−55	17	2.98
−53	−35	−9	2.99	Middle Temporal Gyrus	53	−25	−6	3.28
−51	−33	−17	3.32	Inferior Temporal Gyrus	47	−42	−17	2.99
				Parahippocampal Gyrus	30	−44	−7	4.18
−7	−69	28	3.00	Precuneus	9	−65	42	2.98
−10	−11	47	3.06	Posterior Cingulate	9	−66	11	4.29
INCREASE		Left Hemisphere					Right Hemisphere	
−56	−14	32	3.29	Pre-Central Gyrus	52	−1	30	4.68
−12	7	12	3.30	Caudate	8	6	16	3.29
−17	6	−10	3.01	Putamen	31	−11	−3	3.75
−56	−23	33	4.04	Inferior Parietal Lobule				
				Middle Occipital Gyrus	38	−77	1	2.99

Table 5

Correlations between Change in Glucose Metabolism During Citalopram Treatment and Hamilton Depression Rating Scale (HDRS) Ratings

NEGATIVE		**Left Hemisphere**					**Right Hemisphere**	
	Talairach Coordinates					**Talairach Coordinates**		
x (mm)	**y (mm)**	**z (mm)**	**Z score**	**Structure**	**x (mm)**	**y (mm)**	**z (mm)**	**Z score**
−4	1	29	3.92	Anterior Cingulate Gyrus	9	−22	37	3.52
				Middle Frontal Gyrus	18	43	21	3.65
				Superior Temporal Gyrus	52	−59	25	3.57
				Middle Temporal Gyrus	55	−14	−19	3.85
				InferiorTemporal Gyrus	57	−57	−14	3.56
−44	−52	−18	3.39	Fusiform Gyrus				
−6	−66	51	−3.06	Precuneus	1	−61	43	3.61
Positive		Left Hemisphere					Right Hemisphere	
−24	−69	43	3.06	Superior Parietal Lobule				
−52	−45	25	3.89	Inferior Parietal lobule	52	−38	26	3.56
				Cuneus	10	−94	6	3.28